Electronic Supplementary Material (ESI) for ChemComm.

Supporting Information

for

Polymorphism Control of an Active Pharmaceutical Ingredient Beneath Calixarene-based Langmuir Monolayers

Ludovico G. Tulli,[a] Negar Moridi,[a] Wenjie Wang,[b] Kaisa Helttunen,[c] Markus Neuburger,[d] David Vaknin,[b] Wolfgang Meier,[d] and Patrick Shahgaldian[a*]

[a]Institute of Chemistry and Bioanalytics, School of Life Sciences, University of Applied Sciences Northwestern Switzerland, Muttenz, Switzerland

[b]Ames Laboratory, and Department of Physics and Astronomy, Iowa State University, USA

[c]Department of Chemistry, Nanoscience Center, University of Jyväskylä, Finland

[d]Department of Chemistry, University of Basel, Switzerland

Table of contents

Experimental

General

5,11,17,23-tetra-carboxy-25,26,27,28-tetradodecyloxycalix[4]arene (**1**) was synthesized as previously described.[1] The analytical data were in perfect agreement with that reported. Analytical grade chloroform, dichloromethane, methanol and pyridine were purchased from Sigma-Aldrich and used without further purification. Nanopure water (resistivity ≥ 18 MΩ.cm) was produced with a Millipore Synergy purification system. Gabapentin was purchased from AK Scientific and used without further purification. Infrared spectra were collected in attenuated total reflection (ATR) using a single reflection diamond ATR device (Golden Gate) and a Varian 670-IR spectrometer.

Langmuir isotherms

Langmuir isotherms experiments were carried out using a Nima 112D system. The Langmuir trough was cleaned with analytical grade dichloromethane and nanopure water (resistivity ≥ 18 MΩ·cm) prior to use. Solutions of **1** were prepared by dissolving the appropriate amount of the amphiphile in chloroform (5% methanol) at the concentration of 1 g L^{-1}. Ten μL of solutions of **1** were spread at the water surface using a gastight microsyringe. The monolayer was allowed to stand for 20 minutes for the total evaporation of the solvent and the stabilization of the surfactants at the interface. The monolayer was compressed in a symmetric two-barriers continuous mode at a speed rate of 5 cm^2 min^{-1}. Aqueous GBP solutions were prepared extemporaneously using nanopure water.

Brewster angle microscopy (BAM) and spectroscopic imaging ellipsometry

BAM micrographs were aquired out using a Nanofilm_ep3 system (Accurion) and a Langmuir-Blodgett trough (Nima 112). An internal solid-state laser was used as light source (wavelength: 658 nm); the micrographs were acquired using a CCD camera (768 x 562 pixels) and a 10x objective equipped with an automatic focus scanner. The lateral resolution was 1 μm. Ellipsometry measurements were carried out using the same system in a nulling PCSA (polarizer-compensator-sample-analyzer) set-up. The linear polarizer (P) and the quarter-wave plate (C) yielded an elliptically polarized incident beam that was reflected to the analyzer (A). The variation of the angle for P, C and A allowed fulfilling the Null conditions for the analyzed samples. Eighty μL of solutions of **1** were spread at the water surface using a microsyringe. The monolayer was allowed to stand for 20 minutes for the total evaporation of the solvent and the stabilization of the surfactants at the interface.

Crystallization experiments

The crystallization experiments were performed in scintillation vials spreading appropriate volumes of solutions of **1** at the surface of supersaturated aqueous solutions of GBP (150 g L^{-1}). The solubility of GBP in water was evaluated at 22 °C by adding minute amounts of the API to a volume of nanopure water. GBP appeared to precipitate at a concentration of 144 g L^{-1}. Each condition was repeated ten times to ensure the reproducibility of the experiments. Two controls were used; one spreading only chloroform at the surface in order to ensure that the crystal growth was not dependent on the endothermic evaporation of the solvent and the other one having only the supersaturated aqueous GBP solution. The so-prepared solutions were allowed to stand at 22 °C and after 14 days, millimeter- to centimeter-sized crystals were present in all the crystallization vials where **1** was spread on the aqueous solution surface, strictly confined to the air-liquid interface.

X-ray reflectivity and grazing incidence X-ray diffraction measurements

X-ray reflectivity (XR) and grazing incidence X-ray diffraction (GIXD) of monolayers of **1** were carried out on the liquid surface spectrometer (LSS) using synchrotron radiation (X-ray energy E = 13.474 keV, wavelength λ = 0.92107 Å) at sector 9ID-C, Advanced Photon Source (APS), Argonne National Laboratory. Solutions of **1** were prepared by dissolving the appropriate amount of the amphiphile in chloroform (5% methanol) at a concentration of 1 g L^{-1}. 50 μL of solutions of **1** were spread at the water surface and compressed on a Teflon Langmuir trough contained in an air-tight canister that was purged with water-saturated helium.[2] The scattering vector (wavevector transfer), **Q**, is defined as $\mathbf{k_f} - \mathbf{k_i}$, where $\mathbf{k_i}$ and $\mathbf{k_f}$ represent the wavevectors of the incident and scattered beam, respectively. In reflectivity measurements, the incident angle (α) and the exit angle (β) of the beam with respect to the liquid surface are set equal and the azimuthal angle $\varphi_{xy} = 0$ (φ_{xy} defined as the in-plane angle between the projection of the exit beam on the liquid surface and the incident plane). The reflectivity, R, is a function of the z-component of **Q**, Q_z ($Q_z = 4\pi\sin(\alpha)\lambda^{-1}$), and is related to the electron density (ED), $\rho(z)$, across the interface along the z-axis along the surface normal.[2] A parameterized multi-slab model using Parratt's recursive method[3] are used to extract the ED from the reflectivity data. The GIXD is used to determine the two-dimensional (2D) in-plane ordering and correlations in the monolayer.[2] The GIXD measurements were conducted with a vertically mounted position sensitive detector (PSD), as the function of the in-plane component of **Q**, Q_{xy} ($Q_{xy} \sim 4\pi \sin(\varphi_{xy} 2^{-1}) \lambda^{-1}$.[2] In this study, the incident angle α was kept at 0.065° that is below the critical angle for total reflection,

α_c (α_c = 0.091°), which corresponds to a penetration depth of X-ray ~ 50-100 Å normal to the surface. More experimental details can be found elsewhere.[2, 3, 4]

Single crystal X-ray diffraction

Anhydrous gabapentin polymorphic forms α and ɣ and hydrate gabapentin polymorphic form I have been identified by determination of the unit cell parameters on a Bruker KappaAPEX diffractometer using the APEX2 data collection software.[5]

Single crystals of **1** were crystallized from pyridine. A suitable crystal was measured on a SuperNova, Dual, Cu at zero, Atlas diffractometer using mirror monochromatized CuK_α (λ = 1.5418 Å) radiation at a temperature of 120.01(10) K. The structure was solved with the olex2.solve structure solution program (Charge Flipping) in Olex2 software,[6] and refined with the XL refinement[7] package using Least Squares minimization and SHELX-97 package. The hydrogen atoms were calculated to their idealized positions with isotropic temperature factors (1.2 or 1.5 times the C temperature factor) and refined as riding atoms, except OH hydrogen atoms, which were located from the electron density map and restrained using DFIX 0.82. One of the carboxylic acid groups was disordered (C80, O11, O12; site occupancies 0.68:0.32) and OH of the less occupied site was calculated to the idealized position on O12B. OH on O6 was disordered over two positions H6:H5 (0.5:0.5). Two of the dodecyl chains were modeled as disordered over two positions: C29-C32 with site occupancies of 0.78:0.22, and C65, C68 and C70 with site occupancies of 0.53:0.47. Restrains SADI, DELU and SIMU, and EADP constrain were used, when necessary. Residual electron density (0.84 e $Å^{-3}$) was located at 0.97 Å from C65 causing a B-level alert in checkcif. For C72-C76 vibration perpendicular to chain axis induced elongated ellipsoids and shorter C-C bond lengths than expected, regardless of DFIX 1.54 restrain (B- and C-level errors in checkcif). Three disordered pyridine moieties were located from the electron density with site occupancies N100-C105:N104-C109, 0.5:0.5; N124-C129:N118-C123, 0.63:0.37; N130-C135:N136-C140, 0.73:0.27. The pyridine moieties were restrained using FLAT, SADI, DELU and SIMU, or constrained using AFIX 66 or EADP, when necessary. Building a disorder model for pyridine C112-C117 was attempted but it did not improve the structure. In addition, continuous electron density corresponding approximately to one pyridine moiety was included between layers of **1**. No reasonable disorder model was found for this electron density, and it was removed from the later stage of refinement using solvent mask option in Olex2 (see checkcif). Crystallographic data (excluding structure factors) for the structures in this paper have been deposited with the Cambridge Structural

Data Center as supplementary publication no. CCDC973532. Copies of the data can be obtained free of charge from The Cambridge Crystallographic Data Centre via www.ccdc.cam.ac.uk/data_request/cif.

Crystal structures of 1

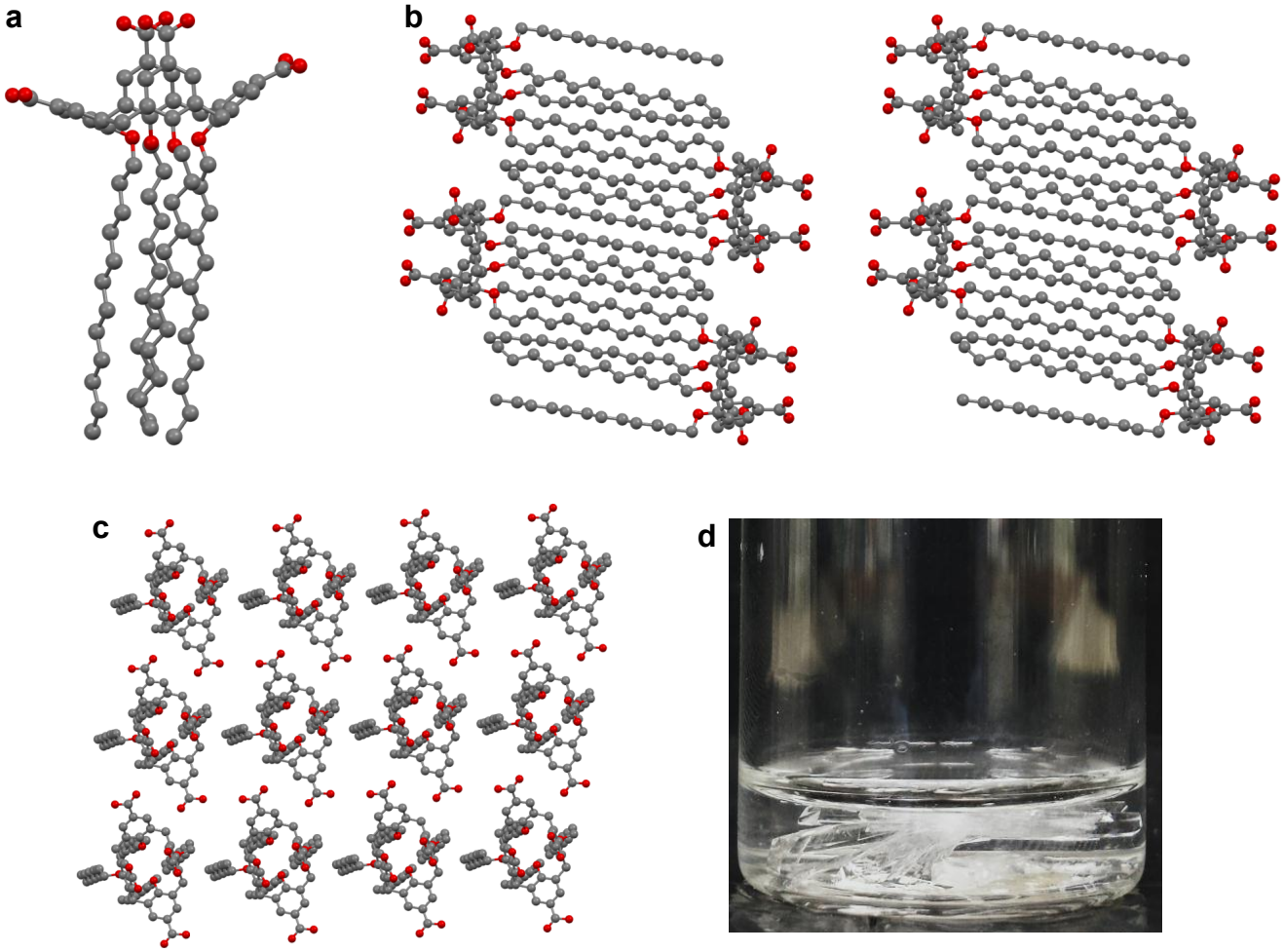

Fig. S1 Solid-state structures of **1** (**a**: single crystal structure of **1**, **b**: packing arrangement along *b*, **c**: packing arrangement along *c*), and **d**: representative photograph of a GBP crystal grown beneath a monolayer of **1**. Solvent molecules and hydrogen atoms are omitted for clarity.

Crystal Data for $C_{80}H_{120}O_{12}\cdot(C_5H_5N)_5$ (**1**) (M =1669.26): triclinic, space group P -1 (no. 2), a = 12.0887(3) Å, b = 12.9462(3) Å, c = 32.3959(8) Å, α = 96.255(2)°, β = 94.2284(19)°, γ = 98.8577(19)°, V = 4958.6(2) Å^3, Z = 2, T = 120.01(10) K, μ (Cu K$_\alpha$) = 0.567 mm^{-1}, D_{calc} = 1.118 g mm^{-3}, 33020 reflections measured (6.96 ≤ 2θ ≤ 153.16), 19903 unique (R_{int} = 0.0153) which were used in all calculations. The final R_1 was 0.0839 (>2σ (I)) and wR_2 was 0.2779 (all data).

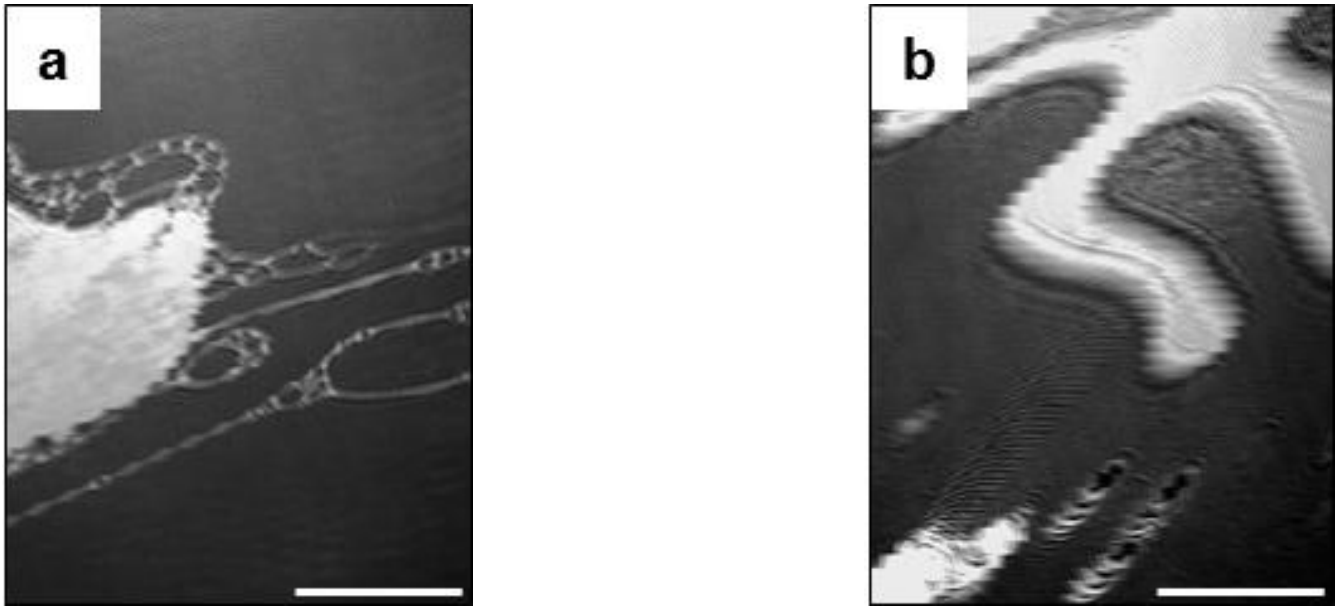

Fig. S2 BAM micrographs of monolayers of **1** on pure water (**a**) and on a 5 g L^{-1} aqueous GBP subphase (**b**) at a value of surface pressure of π = 0 mN m^{-1}. Scale bar = 100 μm.

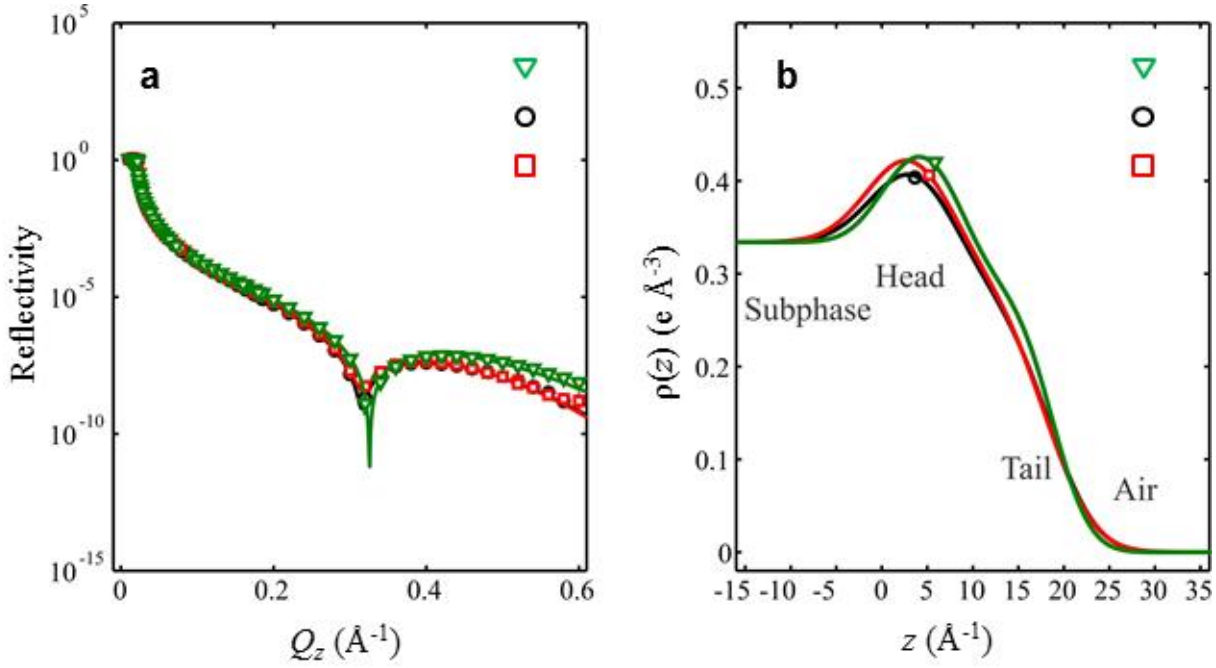

Fig. S3 a) Reflectivity data of monolayers of **1** on pure water (▽ π = 25 mN m^{-1}, ○ π = 45 mN m^{-1}) and on 5 g L^{-1} aqueous GBP subphase (□: π = 45 mN m^{-1}). The oscillatory behavior, and the minimum at Q_z ~ 0.30 Å^{-1}, unequivocally indicate the presence of a monolayer at the vapor/water interface. Qualitatively, the reflectivity data for various conditions almost coincide within the measured Q_z range (up to 0.7 Å^{-1}) suggesting the ED profiles along the surface normal are not significantly different. The difference at the high Q_z end, i.e. higher reflectivity at low value of surface pressure, can be accounted for by the lower surface roughness as expected from capillary-wave theory.[2, 3] **b**) Corresponding best-fit ED profiles.

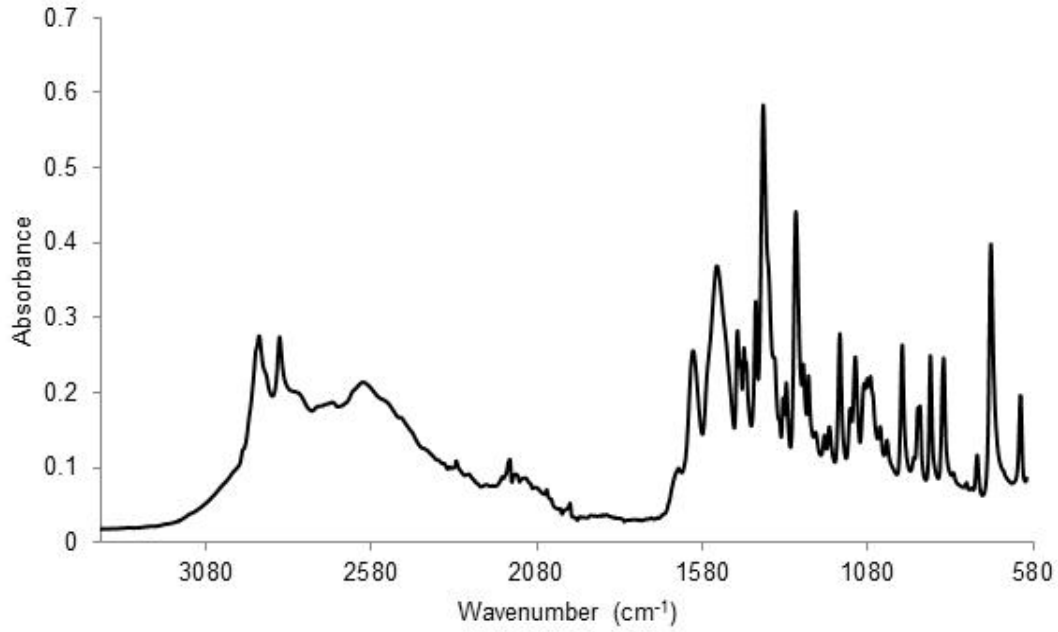

Fig. S4 Infrared spectrum of GBP polymorphic form α (π = 45 mN m^{-1}).

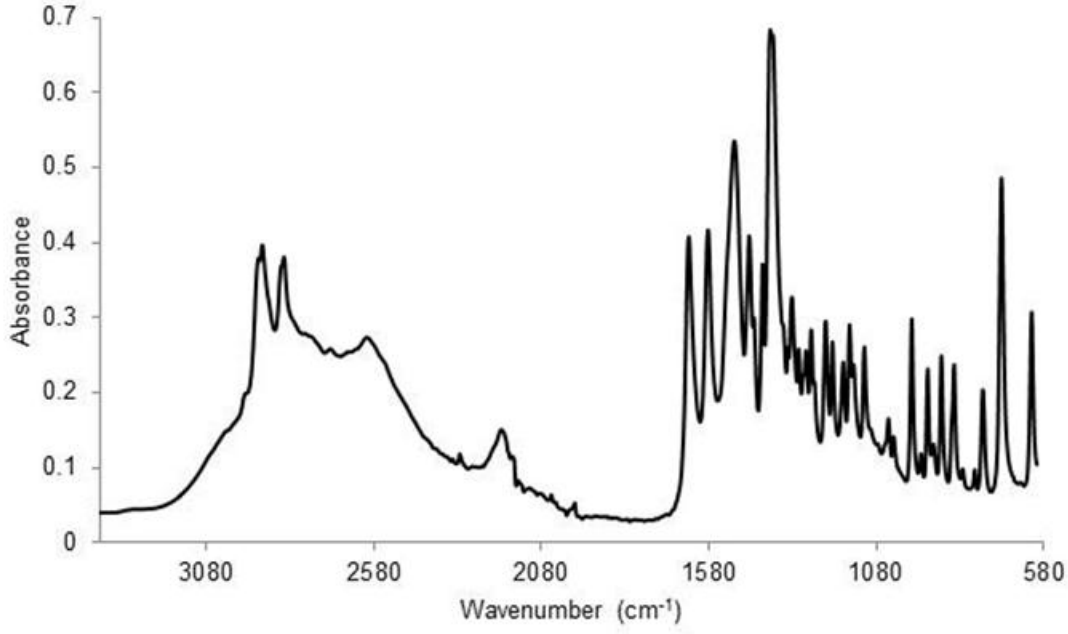

Fig. S5 Infrared spectrum of GBP polymorphic form ɣ (π = 0, 1 and 25 mN m^{-1}).

References:

1 N. Moridi, O. Danylyuk, K. Suwinska, and P. Shahgaldian, *J. Colloid Interface Sci.*, 2012, **377**, 450-455.

2 D. Vaknin, in *Characterization of Materials*, John Wiley & Sons, 2012, pp. 1-32.

3 J. Als-Nielsen, D. McMorrow, in *Elements of Modern Physics*, John Wiley & Sons, 2011, pp. 69-112.

4 W. Wang, N. S. Murthy, I. Kuzmenko, N. A. Anderson, D. Vaknin, *Langmuir*, 2013, **29**, 11420-11430.

5 *Apex 2: Version 2 User Manual, M86-E01078*, Bruker Analytical X-ray Systems, 2006.

6 O. V. Dolomanov, L. J. Bourhis, R. J. Gildea, J. A. K. Howard, H. Puschmann, *J. Appl. Cryst.*, 2008, **42**, 339-341.

7 G. M. Sheldrick, *Acta Crystallogr., Sect. A: Found. Crystallogr.*, 2008, **64**, 112-122.